Applied Catalysis B: Environmental 89 (2009) 123–127

Contents lists available at ScienceDirect

Applied Catalysis B: Environmental

journal homepage: www.elsevier.com/locate/apcatb

Effect of chromium migration from metallic supports on the activity of diesel exhaust catalysts

W. Kaltner, M. Veprek-Heijman, A. Jentys *, J.A. Lercher

Department Chemie, Technische Universität München, Lichtenbergstraβe 4, 85748 Garching, Germany

ARTICLE INFO

Article history:
Received 25 August 2008
Received in revised form 1 December 2008
Accepted 6 December 2008
Available online 24 December 2008

Keywords:
Metallic support structures
Oxidation catalysts
Cr diffusion

ABSTRACT

Fe–Cr–Ni and Fe–Cr–Al sintered spheres are explored as alternative support structures for automotive exhaust catalysts. Initially the activity of Pt supported on the metal support and on ceramic monoliths (cordierite) for the oxidation of CO and NO is comparable. However, after thermal aging at elevated temperatures (800 °C) and extended reaction times (24 h) the activity for the oxidation of NO of the catalysts supported on the Fe–Cr–Ni spheres decreases significantly, which is attributed to the migration of chromium from the metal bulk phase into washcoat. In the contrary, the aluminium present in the Fe–Cr–Al steel alloy formed a protective alumina barrier inhibiting the degradation of the catalyst after aging by blocking the migration of chromium to the surface.

1. Introduction

Catalytic converters for the oxidation of CO and residual hydrocarbon emissions are necessary for diesel cars to comply with current emission legislation. In typical diesel oxidation catalysts platinum supported on ceramic or metallic monoliths is used as active component for the oxidation of CO, NO and hydrocarbons [1,2]. Recently, novel structures based on stainless steel hollow spheres [3] were proposed as catalyst supports for future applications, having the potential to combine different functionalities such as catalysis and noise reduction.

While most studies of diesel oxidation catalysts have investigated reaction mechanisms and tried to improve the catalytic activities properties of the fresh catalysts, the deactivation during long-term application at elevated temperatures has not been studied in great detail. In general, the following processes for deactivation of exhaust catalyst have been reported [4–10]: (i) loss of metal surface area due to sintering of Pt after long-term operation at high temperature (thermal deactivation), (ii) accumulation of poisons such as Ca and P arising from the lubricant oil on the surface of the active sites, (iii) formation of sulfates from sulfur species in the fuel, (iv) coking and (v) the migration or diffusion of elements such as Cr from the support into the washcoat or into the active noble metal phase. The deactivation depends strongly on the combination of parameters such as time, temperature, atmosphere, support and catalyst composition.

In the present study Pt-based oxidation catalysts supported on metallic hollow sphere structures and on a ceramic monolith are thermally aged under laboratory conditions. The light-off temperature for the CO oxidation and the activity for NO oxidation were used as indicators for the catalytic activity. Both are typical reactions for the emission reduction in car exhaust systems. The CO oxidation is required to lower the emissions, while the oxidation of NO to NO_2 is used to enhance the rate in a subsequent NH_3-SCR reaction [11] and for the effective removal of soot from a particulate filter [12].

2. Experimental

2.1. Catalysts

The support structures were of cylindrical shape. For catalyst A (diameter 21 mm × length 25 mm) and catalyst B (diameter 21 mm × length 28 mm) sintered hollow sphere structures (sphere diameter of 3 mm) made of Fe–Cr–Ni and of Fe–Cr–Al stainless steel, respectively, were used (for compositions see Table 1) as support. The hollow spheres were prepared by coating PE spheres with metal particles, followed by a thermal treatment to remove the inner core and to sinter the particles to a stable shell. These intermediates were packed into the desired shape (e.g. a torus or a sheet) and sintered to obtain the final structure. For catalyst C (diameter 21 mm × length 25 mm) a ceramic monolith (cordierite 400 cpsi) was used as support.

The metallic structures were pre-treated in air at 680 °C, coated with a standard washcoat based on γ-Al_2O_3 and impregnated with Pt (loading 3.5×10^3 g/m^3), a formulation typically used for diesel

* Corresponding author. Tel.: +49 89 289 135 38; fax: +49 89 289 135 44.
E-mail address: Andreas.Jentys@ch.tum.de (A. Jentys).

0926-3373/$ – see front matter © 2008 Elsevier B.V. All rights reserved.
doi:10.1016/j.apcatb.2008.12.006

Table 1
Composition of the metallic support structures.

wt%	Catalyst A (Fe–Cr–Ni)	Catalyst B (Fe–Cr–Al)
Cr	24–26	19–22
Ni	19–22	–
Mn	<2	<1
Si	1.5–2.5	<1
C	<0.2	<0.1
S	0.03	0.03
P	0.045	0.045
Al	–	5
O	<0.1	–
Fe	Balance	Balance

oxidation catalysts [2,13]. The washcoat was applied by a standard dipping method, where the speed for the removal of the structure from the slurry and the removal of the excess slurry were controlled. Dipping and calcining were repeated until the desired amount of washcoat was applied onto the structure.

2.2. Catalytic test reactions

The oxidation of NO and CO were studied in a flow reactor, the concentration of products was continuously analyzed by IR spectroscopy (FTIR Thermo Electron Corporation NEXUS, OMNIC QuantPad software) using a heated, low volume multiple-path gas cell. The reactions were carried out using a gas stream consisting of 4000 ml/min N_2 (carrier gas), 50 ml/min O_2 and 4 ml/min NO or CO, which corresponds to a NO or CO concentration of 1000 ppm and an O_2 concentration of 2.5%. The space velocity over the catalyst was 70,000 h^{-1}. During the experiments, the temperature was increased from room temperature to 550 °C using an increment of 1 °C/min, while continuously monitoring the temperature before and after the catalyst and the concentration of products and reactants. Aging of the catalysts was carried out in the reactor at 800 °C for 48 h under synthetic air.

2.3. X-ray photoelectron spectroscopy (XPS)

Photoelectron spectra were recorded on a Leybold LH10 system using Al Kα radiation (1486.6 eV). The analysis chamber was operated under ultrahigh vacuum with a base pressure of 4×10^{-9} mbar. The binding energies were referenced to the C 1s peak at 284.9 eV typically present due to adventitious carbon. The intensities of the following peaks were used for quantitative analysis: Al 2s, O 1s, C 1s, Fe $2p^3$, Cr $2p^3$, Pt 4f, and Pt 4d. Peak areas were determined using Shirley background subtraction and for the quantitative analysis sensitivity factors from ref. [14] were used.

2.4. Scanning electron microscopy (SEM)

A JEOL 500 instrument with an accelerating voltage of 25 kV was used. Energy dispersive X-ray spectroscopy was used for the characterization of Cr distribution in the samples.

3. Results

3.1. Effect of the aging process on the activity for oxidation of NO and CO

A typical conversion profile for CO and NO over catalyst B is shown in Fig. 1, the latter is limited by the thermodynamic equilibrium between NO and NO_2. Therefore, the NO conversion increases with the temperature and after the NO_2 concentration reaches the thermodynamic equilibrium the conversion follows the equilibrium concentration [2,13,15–17]. In contrast

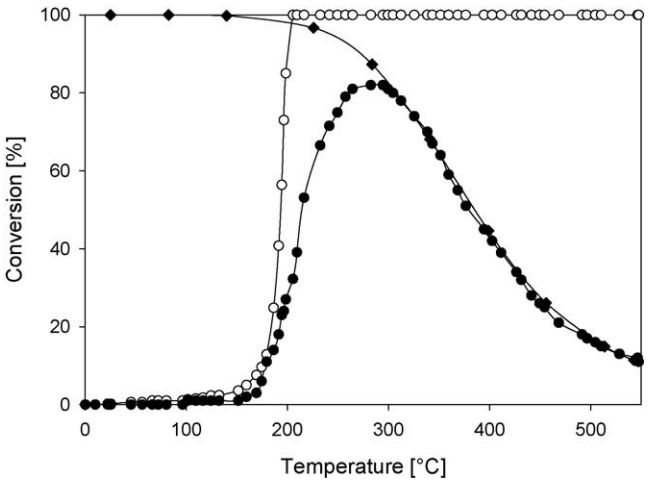

Fig. 1. Conversion of (○) CO and (●) NO for Pt supported Fe–Cr–Al (catalyst B), (◆) thermodynamic equilibrium between NO + (1/2)O_2 and NO_2.

the CO conversion is not limited by an equilibrium, therefore, the conversion reaches 100% [18].

The (differential) rates for the oxidation of NO at 200 °C and the light-off temperatures for the CO oxidation (temperature for 50% CO conversion) were used to evaluate the activity of the catalysts. The rates for the oxidation of NO of monolith and hollow sphere catalysts before and after aging the catalyst structures are compared in Fig. 2. Catalyst A showed the lowest activity for NO oxidation (rate 2.07×10^{-3} μmol s^{-1} $g_{Pt}{}^{-1}$) followed by catalyst B (2.26×10^{-3} μmol s^{-1} $g_{Pt}{}^{-1}$) and catalyst C (2.50×10^{-3} μmol s^{-1} $g_{Pt}{}^{-1}$). After thermal aging at 800 °C for 48 h under synthetic air, the activity for the NO oxidation generally decreases due to sintering of Pt particles on the surface. Catalysts C and B showed almost the same activity after aging (decrease of 27% and 32%, respectively), whereas the activity of catalyst A significantly decreased (53% loss of activity).

The light-off temperatures for the CO conversion over the catalysts before and after thermal aging are compared in Fig. 3 [19–21]. Catalysts on the hollow sphere structures (catalysts A and B) showed a lower light-off temperature (190 °C) compared with the cordierite monolith support (210 °C). After the aging the light-off temperature increased for catalyst A to 220 °C, for catalyst B to 210 °C (slightly more active) and for catalyst C to 220 °C.

3.2. Testing for mass transport limitations

The existence of external mass transfer limitations was investigated for catalysts B and C by measuring the conversion

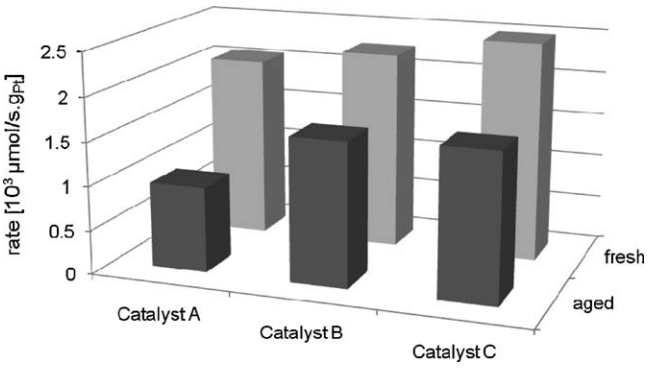

Fig. 2. Rate of NO oxidation at 200 °C.

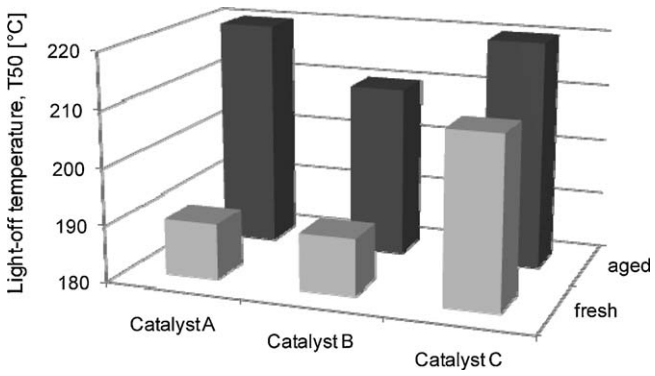

Fig. 3. CO light-off temperature.

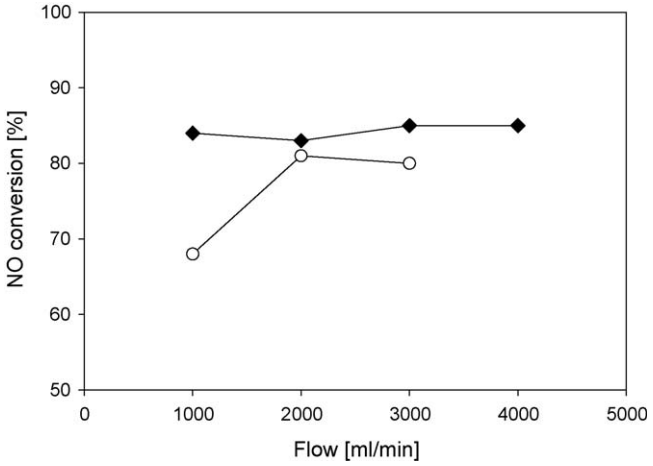

Fig. 4. Conversion of NO as function of the residence time for (◆) hollow sphere structure and (○) ceramic monolith.

of NO as function of the flow, while maintaining constant residence time by increasing the catalyst length (see Fig. 4).

In the flow range studied (1000–4000 ml/min) constant NO conversion was observed for the hollow sphere structures, indicating that the mass transport in the film did not influence the reaction rate. In contrast, at lower flow rates transport limitations from film diffusion were observed for the monolithic structure.

3.3. Washcoat thickness for hollow sphere supports

Sintered metal foils with the same composition alloys as the hollow sphere supports (Fe–Cr–Ni and Fe–Cr–Al) were coated with an alumina-based washcoat and used as model catalysts for the XPS measurements. The preparation method and the washcoat composition was the same as for the hollow sphere structures. The thickness of the oxide layer was measured by scanning electron microscopy (see Fig. 5), for both supports a washcoat thickness of 20 μm was determined. Moreover, both surfaces revealed distinct cracks, which result from the thermal treatment during calcination. Additionally, the structural properties of the washcoat layer on hollow spheres were investigated by X-ray tomography, which indicated a thickness of 11 μm [22].

3.4. Influence of chromium on the surface of Fe–Cr–Ni stainless steel

The concentration of Cr on the foils coated with the alumina-based washcoat was determined by energy dispersive X-ray analysis. The SEM of the hollow sphere structure of catalyst A after

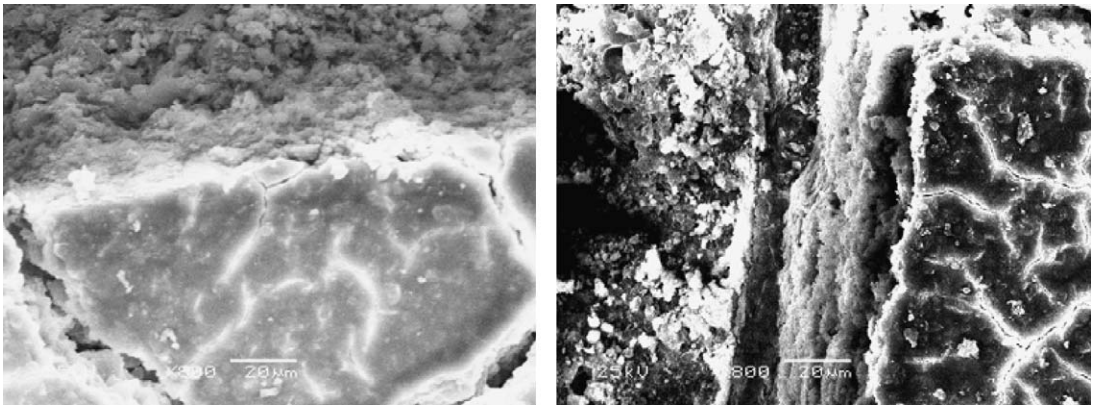

Fig. 5. SEM of washcoat surface on Fe–Cr–Ni and on Fe–Cr–Al foils.

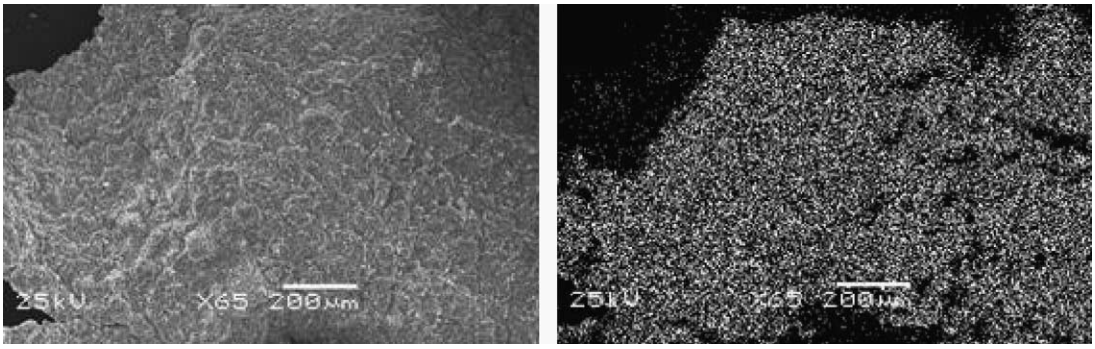

Fig. 6. SEM and EDX mapping of Cr after aging.

Table 2
Washcoat composition of catalyst A and catalyst B before and after aging.

wt%	Catalyst A		Catalyst B	
	Fresh	Aged	Fresh	Aged
O	53.9	56.1	53.2	56.7
C	8.5	7.9	6.8	6.2
Ce	2.2	2.5	2.1	1
Al	34.7	32.7	37.4	36
Pt	0.7	0.4	0.5	0.1
Cr	0	0.4	0	0

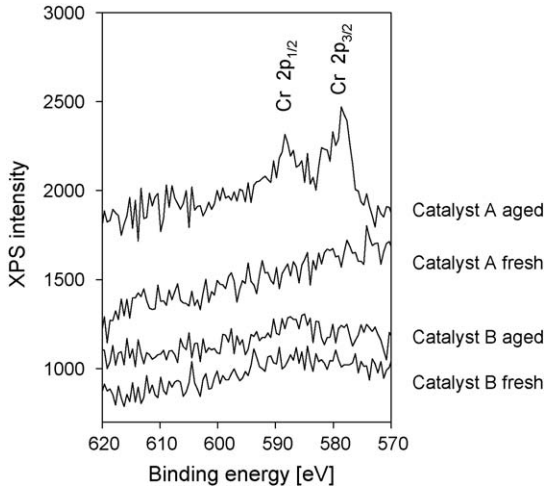

Fig. 7. XPS for catalysts A and B before and after aging.

aging and the Cr mapping from EDX are shown in Fig. 6, which indicates that Cr is distributed over the whole surface of catalyst A. In contrast EDX revealed the absence of Cr on the surface of catalyst B.

To confirm the migration of Cr onto the surface during the thermal aging process XPS were recorded for the sintered foils of catalysts A and B after coating with the washcoat and after the aging process. For both model catalysts a similar composition of the washcoat was observed by XPS before aging (see Table 2). The formation of a thin Al_2O_3 film on the surface of the Fe–Cr–Al alloy of catalyst B during the pre-treatment led to a change in the color of the surface from grey to light-blue, as the preferred phase on the surface of Fe–Cr–Al alloys at high temperature is alumina, in contrast to chromia for Fe–Cr–Ni alloy used for catalyst A [9,23]. The XPS for catalysts A and B before and after thermal aging are compared in Fig. 7. The XPS peaks at 580–590 eV confirm the presence of Cr^{3+} on the surface of the aged Fe–Cr–Ni catalyst, whereas on the fresh catalyst A, as well as on the fresh and aged catalyst B, Cr was not detected on the surface.

4. Discussion

The activity of Pt-based oxidation catalysts supported on hollow sphere structures for the oxidation of NO and CO was comparable to that of Pt supported on cordierite monoliths [24,25]. Transport limitations by film diffusion were not found for the hollow sphere supports, which is an advantage compared to monolithic structures with straight pores, where external mass transport limitations are frequently observed under typical reaction conditions [25,26].

After thermal aging at 800 °C the activity for the oxidation of CO and NO decreased for the catalysts on the metallic as well as on the oxidic supports. For CO oxidation the light-off temperature was only slightly affected, while the activity for NO oxidation was more sensitive to the thermal aging. For the Fe–Cr–Al support (catalyst B) and for the cordierite monolith (catalyst C) the activity decreased by 30%, while more than 50% decrease in the rate of NO oxidation was observed for the Fe–Cr–Ni supported catalyst (catalyst A). This difference is attributed to the migration of Cr from the bulk phase of the support onto the catalysts surface forming Cr_2O_3 species. As the noble metal particles are the active species for CO and NO oxidation the decrease in activity indicates that further diffusion/migration of Cr^{3+} from the washcoat into the metal appears to be feasible at the temperatures used. The accumulation of Cr^{3+} on the surface of catalyst A after aging for Fe–Cr–Ni support (catalyst A) is clearly shown by XPS and EDX mapping. Both experiments indicated that Cr was diffusing from the stainless steel support (Fe–Cr–Ni) through the washcoat to the surface for catalyst A. In contrast Cr could not be detected after the thermal aging of catalysts B and C.

In principle, Cr diffusion should be also possible from the Fe–Cr–Al alloy used in catalyst B. The difference between the Fe–Ni–Cr and the Fe–Cr–Al alloy is that at high temperatures (~1000 °C) the Fe–Cr–Ni alloy forms a Cr_2O_3 phase on the surface, whereas the Fe–Cr–Al alloy forms a dense Al_2O_3 phase, which prevents further migration of Cr. After the thermal pre-treatment of catalyst B, the color of the alloy changed from grey to light-blue, which indicates the formation of the protective alumina layer on the surface.

In order to confirm the role of Cr^{3+} on the activity for the oxidation of NO an experiment with an aged monolithic structure, which was impregnated with a Cr-solution, was carried out. As this catalyst did not show any activity for the oxidation of NO, the poising effect of Cr was confirmed.

The detrimental influence of Cr^{3+} on the activity of the noble metal might be explained in analogy to metalcarbonyles. NO is a stronger acceptor of backbonding electrons than CO. If NO binds to the metal, the additional electron of the NO radical is transferred completely to the metal atom, therefore, a nitrosyl ion is formed which is isoelectronic to CO. The extra electron provided by NO results in a stronger backbonding compared to CO. If Cr is present on the surface, only CO can be oxidized to CO_2, while NO binds to the surface without further reaction. Therefore the oxidation of CO is not influenced by Cr on the surface, but the NO oxidation rate is reduced because less active sites are available.

5. Conclusions

Similar catalytic activity was reached in the oxidation of NO to NO_2 and CO to CO_2 with the hollow sphere supports compared to traditional corderite supports. However, caution is necessary in case of constant high temperature applications, which can lead to the migration of chromium from the support through the washcoat to the surface which causes a loss of activity for Fe–Cr–Ni alloys. Improvement of the stainless steel, changing the support structure to Fe–Cr–Al with low aluminum content, resulted in the growth of a protective alumina barrier during the pre-oxidation process.

Acknowledgement

This work was supported by the Bundesministerium für Bildung und Forschung (BMBF) under the WING initiative (project number 03X3004). SEM and EDX measurements were done by M. Neukamm at the Chair of Technical Chemistry II at TUM Garching.

References

[1] H.J. Stein, Appl. Catal. B 10 (1996) 69.
[2] P.J. Schmitz, R.J. Kudla, A.R. Drews, A.E. Chen, C.K. Lowe-Ma, R.W. McCabe, W.F. Schneider, C.T. Goralski, Appl. Catal. B 67 (2006) 246.

[3] O. Andersen, U. Waag, L. Schneider, G. Stephani, B. Kieback, Adv. Eng. Mater. 2 (2000) 192.
[4] J.E. Johnson, D.B. Kittelson, Appl. Catal. B 10 (1996) 117.
[5] J. Andersson, M. Antonsson, L. Eurenius, E. Olsson, M. Skoglundh, Appl. Catal. B 72 (2007) 71.
[6] A.F. Lee, K. Wilson, R.M. Lambert, C.P. Hubbard, R.G. Hurley, R.W. McCabe, H.S. Gandhi, J. Catal. 184 (1999) 491.
[7] A.K. Neyestanaki, F. Klingstedt, T. Salmi, D.Y. Murzin, Fuel 83 (2004) 395.
[8] S. Albertazzi, P. Arpentinier, F. Basile, P. Del Gallo, G. Fornasari, D. Gary, A. Vaccari, Appl. Catal. A 247 (2003) 1.
[9] J. Sainio, A. Aronniemi, O. Pakarinen, K. Kauraala, S. Airaksinen, O. Krause, J. Lahtinen, Appl. Surf. Sci. 252 (2005) 1076.
[10] S. Gudlavalleti, T. Ros, D. Lieftink, Appl. Catal. B 74 (2007) 251.
[11] M. Köbel, M. Elsener, G. Madia, Ind. Eng. Chem. Res. 40 (2001) 52.
[12] J.A. Sullivan, O. Keane, Catal. Today 114 (2006) 340.
[13] R. Burch, A. Ramli, Appl. Catal. B 15 (1998) 63.
[14] C. Wagner, Practical Surface Analysis, vol. 1, Wiley, Chichester, 1990.
[15] L. Ilieva, G. Pantaleo, I. Ivanov, A.M. Venezia, D. Andreeva, Appl. Catal. B 65 (2006) 101.
[16] R. Burch, P. Fornasiero, T.C. Watling, J. Catal. 176 (1998) 204.
[17] M. Crocoll, S. Kureti, W. Weisweiler, J. Catal. 229 (2005) 480.
[18] R. Burch, A. Ramli, Appl. Catal. B 15 (1998) 49.
[19] G. Groppi, E. Tronconi, Chem. Eng. Sci. 55 (2000) 2161.
[20] H. More, R.E. Hayes, B. Liu, M. Votsmeier, M.D. Checkel, Top. Catal. 37 (2006) 155.
[21] N.P. Siswana, D.L. Trimm, Catal. Lett. 46 (1997) 27.
[22] W. Kaltner, K. Lorenz, B. Schillinger, A. Jentys, J.A. Lercher, in press.
[23] P.C. Snijders, L.P.H. Jeurgens, W.G. Sloof, Surf. Sci. 496 (2002) 97.
[24] F. Dorado, A. de Lucas-Consuegra, P. Vernoux, J.L. Valverde, Appl. Catal. B 73 (2007) 42.
[25] E. Tronconi, Catal. Today 34 (1997) 421.
[26] E. Tronconi, A. Beretta, Catal. Today 52 (1999) 249.